HHS Public Access

Author manuscript

Sci Transl Med. Author manuscript; available in PMC 2020 June 17.

Published in final edited form as:

Sci Transl Med. 2015 July 08; 7(295): 295ra108. doi:10.1126/scitranslmed.aab1996.

Tmc gene therapy restores auditory function in deaf mice

Charles Askew[1,2], **Cylia Rochat**[3], **Bifeng Pan**[1], **Yukako Asai**[1], **Hena Ahmed**[1], **Erin Child**[1], **Bernard L. Schneider**[3], **Patrick Aebischer**[3], **Jeffrey R. Holt**[1]

[1]Department of Otolaryngology, F.M. Kirby Neurobiology Center, Boston Children's Hospital and Harvard Medical School, Boston, MA 02115, USA [2]Neuroscience Graduate Program, University of Virginia, Charlottesville, VA 22908, USA [3]Brain Mind Institute, École Polytechnique Fédérale de Lausanne, Lausanne, CH-1015 Lausanne, Switzerland

Abstract

Genetic hearing loss accounts for up to 50% of prelingual deafness worldwide, yet there are no biologic treatments currently available. To investigate gene therapy as a potential biologic strategy for restoration of auditory function in patients with genetic hearing loss, we tested a gene augmentation approach in mouse models of genetic deafness. We focused on DFNB7/11 and DFNA36, which are autosomal recessive and dominant deafnesses, respectively, caused by mutations in transmembrane channel–like 1 (*TMC1*). Mice that carry targeted deletion of *Tmc1* or a dominant *Tmc1* point mutation, known as *Beethoven*, are good models for human DFNB7/11 and DFNA36. We screened several adeno- associated viral (AAV) serotypes and promoters and identified AAV2/1 and the chicken b-actin (*Cba*) promoter as an efficient combination for driving the expression of exogenous *Tmc1* in inner hair cells in vivo. Exogenous *Tmc1* or its closely related ortholog, *Tmc2*, were capable of restoring sensory transduction, auditory brainstem responses, and acoustic startle reflexes in otherwise deaf mice, suggesting that gene augmentation with *Tmc1* or *Tmc2* is well suited for further development as a strategy for restoration of auditory function in deaf patients who carry *TMC1* mutations.

Introduction

Hearing loss is the most common sensory deficit in the world, with both genetic and environmental factors causing dysfunction of the primary sensory cells of the inner ear,

Corresponding Author: Jeffrey Holt, PhD, 3 Blackfan Circle, Center for Life Sciences, Rm 3003, Boston, MA 02115, Tel: 617-919-3574, jeffrey.holt@childrens.harvard.edu.

Author contributions: C.A. performed experiments, analyzed data, and helped write the manuscript; C.R. designed and generated vectors; B.P. performed experiments and analyzed data; Y.A. designed and generated vectors, performed experiments, and analyzed data; H.A. performed experiments and analyzed data; E.C. analyzed data; B.L.S. designed and generated vectors and helped design experiments; P.A. helped design vectors and experiments; J.R.H. conceived the study, designed experiments, analyzed data, and helped write the manuscript. All authors critically reviewed and approved the manuscript.

Supplementary Materials
www.sciencetranslationalmedicine.org/cgi/content/full/7/295/295ra108/DC1
Materials and Methods
References (26, 27)

Competing interests: The authors declare that they have no competing interests.

Data and material availability: Plasmids for AAV vector production are available via a material transfer agreement.

known as hair cells (1). Hair cells convert mechanical stimuli into electrical signals and are essential for normal auditory and balance functions. Unfortunately, hair cells lack the ability to regenerate; thus, hair cell damage or death is cumulative, causing progressive hearing loss. The current standards of care for hearing loss are hearing aids or cochlear implants, which provide in- complete restoration of function in a limited patient population. Pharmacologic, stem cell, and gene therapies are being explored as alternative therapies (1). Of these possible strategies, gene therapy may be best suited for restoration of hair cell function in genetic hearing loss (1–4). However, few studies have provided proof-of-principle evidence supporting gene therapy as a viable strategy for restoration of auditory function in mouse models of genetic hearing loss. One notable exception is the restoration of auditory function in mice lacking vesicular glutamate transporter 3 (VGLUT3), a glutamate transport protein ex- pressed in auditory inner hair cells (IHCs), required for synaptic trans-mission from IHC to postsynaptic neurons of the 8th cranial nerve (5). The authors of that study used adeno-associated viral (AAV) vectors to deliver the coding sequence for VGLUT3 into IHCs of early postnatal *Vglut3* knockout mice. Although an important advancement, VGLUT3 mutations are not common in humans and, when present, are dominant, suggesting that the clinical utility of VGLUT3 augmentation may be limited.

To explore gene therapy for a common form of genetic hearing loss that affects hair cells, we used mice that carry mutations in transmembrane channel-like gene 1 (*Tmc1*). Mutations in human *TMC1* account for 4 to 8% of genetic deafness in some populations (6, 7). To date, 40 *TMC1* mutations have been identified that cause deafness in humans (8, 9). Most are recessive and cause prelingual deafness, whereas at least five are dominant and cause progressive hearing loss with onset during the mid-teen years (7), suggesting possible windows of opportunity for clinical intervention.

Although the precise molecular function of TMC1 is unclear, there is agreement that TMC1 and its closely related ortholog, TMC2, affect the permeation properties of sensory transduction channels in auditory hair cells (10–12) and are likely channel components (11). Mice deficient in *Tmc1* and *Tmc2* lack sensory transduction, are deaf, and suffer severe balance dysfunction despite the presence of normal hair cell morphology (10) and hair cells that survive into mature stages (13). Mice that carry the *Beethoven* (*Bth*) (14) point mutation p.M412K in TMC1 retain sensory transduction but have reduced calcium permeability (11). *Beethoven* mice are an excellent model for dominant- progressive hearing loss (DFNA36) in humans who carry an identical substitution in the orthologous position (p.M418K) of the human *TMC1* gene (15). Mice that carry *Tmc1* deletions (10) are good models for recessive hearing loss (DFNB7/11) in humans with loss-of-function mutations in *TMC1*.

Previously, adenoviral vectors were used in vitro to introduce the coding sequence for *Tmc1* or *Tmc2* into hair cells excised from mice deficient in *Tmc1* and *Tmc2* (10). These experiments demonstrated partial restoration of sensory transduction in cultured hair cells in vitro. To extend these studies to an in vivo setting and to develop gene therapy strategies to treat genetic deafness in humans, we designed AAV vectors that carried the coding sequence for *Tmc1* or *Tmc2* and injected them in the ears of *Tmc1* mutant mice. Here, we demonstrate that *Tmc1* and *Tmc2* are functionally redundant, and that either gene can restore sensory transduction and partial auditory function in vivo in mice that carry recessive

Tmc1 mutations. In addition, we used *Tmc2* gene therapy to preserve auditory function and hair cell survival in mice that carried dominant *Bth* mutations in *Tmc1*. Our results support continued development of gene therapy strategies for hearing restoration in humans with genetic deafness.

Results

AAV2/1 targets cochlear hair cells in vitro

To identify AAV serotypes with the highest viral transduction rate in cochlear hair cells, we incubated AAV-*Cmv*-eGFP reporter vectors containing capsid serotypes 1, 2, 6, 8, or 9, at titers that ranged from 3×10^{10} to 4×10^{13} genome copies (gc)/ml, with organotypic mouse cochlear cultures. Green fluorescent protein (GFP)-positive hair cells were evident in all cultures. Confocal images from the mid-basal region of the organ of Corti demonstrated viral transduction of hair cells for each serotype tested at an effective viral concentration of 3×10^{10} to 3×10^{11} gc/ml (Fig. 1A). The total number of hair cells per cochlea ranged from 1575 to 3046, depending on the quality of the dissection, with an average of 2348 ± 389 (±SD; $n = 28$) (Fig. 1B). Quantification of viral transduction rates for whole cochleas revealed that AAV serotype 2/1 transduced the greatest number of hair cells at equivalent viral titers for each serotype. AAV2/1 transduced an average of 58% hair cells along the length of the cochlea, compared with 14% for AAV2/6, the serotype with the next highest viral transduction rate (Fig. 1B).

We noted a tonotopic gradient for viral transduction, apparent for AAV2/1 at all concentrations tested (Fig. 1C), with more total hair cells expressing GFP in the base of the cochlea (up to 95%) than at the apex (up to 54%). The rate of viral transduction of IHCs declined sharply from base to apex (from 81 to 5%; $n = 7$), whereas viral transduction rates in outer hair cells (OHCs) persisted at higher rates along the base-to-apex axis (from 84 to 57%; $n = 7$). The mechanism of the basal-apical gradient is not clear.

Exogenous promoters drive expression in cochlear cultures

Next, we examined the activity of different promoters in cochlear cultures in vitro using the AAV2/1 vector for delivery and enhanced GFP (eGFP) expression as a readout of promoter activity. Promoters were chosen from three different sources that are known to have constitutive activity in most cells types: cytomegalovirus (*Cmv*), chicken b-actin (*Cba*), and mouse phosphoglycerate kinase 1 (*Pgk1*). Additionally, we investigated the activity of the synapsin 1 (*Syn1*) promoter, which is known to be active in cells with synaptic machinery but has not been investigated in hair cells. We found that both *Cmv* and *Cba* promoters drove robust eGFP expression in hair cells, as well as many types of sup- porting cells in the cochlea (Fig. 1D). Surprisingly, although phosphoglycerate kinase is an enzyme present in most cells, the *Pgk1* promoter drove eGFP expression only in supporting cells of the inner sulcus (Fig. 1D). We also observed *Syn1*-driven eGFP expression in spiral ganglion neurons (Fig. 1D), consistent with a recent report in mice (16) and the localization of synapsin protein (17). There was no detectable eGFP expression in IHCs or OHCs despite the presence of ribbon synapses in these cells. Because both *Cmv* and *Cba* drove robust

exogenous gene expression in hair cells, these promoters were chosen for further characterization of AAV2/1 transduction in vivo using eGFP as a reporter.

Round window injection of AAV2/1 targets hair cells

To investigate expression of AAV vectors in the cochlea in vivo, we developed a method for viral delivery to the perilymphatic spaces via round window membrane (RWM) injection into early postnatal mice (P0 to P2). Our RWM injection protocol is similar to other methods (5), except that we left the bulla intact and inserted the micropipette directly through the overlying fascia until it penetrated both the bulla and RWM into the scala tympani. In initial experiments, successful targeting of the perilymphatic spaces was confirmed, where dye-filled turns of the entire cochlea were visually discernible through the bulla.

In the next series of experiments, we injected either AAV2/1-*Cba*- eGFP or AAV2/1-*Cmv*-eGFP unilaterally into the left ear through the RWM of P0 to P2 wild-type mice. When injected ears were harvested at P8 to P10, eGFP fluorescence revealed that both AAV2/1-*Cba*-eGFP (Fig. 2, A **and** B) and AAV2/1-*Cmv*-eGFP (Fig. S1) vectors targeted hair cells and supporting cells and drove transgene expression throughout the cochlea. However, unlike the in vitro results, eGFP was mainly expressed in IHCs in vivo. GFP-positive OHCs were seen sporadically in the basal half of the cochlea, near the injection site, but very few GFP-positive OHCs were found in the apical half of the cochlea (Fig. 2, A **and** B). In cochleas injected with AAV2/1-*Cba*-eGFP, 59 ± 2% (±SD; $n = 2$) of IHCs were eGFP-positive, and with AAV2/1-*Cmv*-eGFP, 70 ± 9% were eGFP-positive ($n = 4$). The utricles of injected mice also displayed eGFP expression in vestibular hair cells and supporting cells (Fig. S2), which confirmed that the injections distributed viral particles throughout the membranous labyrinth. We did not see evidence of GFP expression upon gross inspection of the auditory brainstem or other bodily tissues.

Both *Cmv* and *Cba* drove robust expression of eGFP in hair cells, but we opted to focus on the *Cba* promoter, which has recently been shown effective for driving exogenous *Vglut3* expression in mouse IHCs in vivo (5). To assay for possible deleterious consequences on hair cell function, we measured sensory transduction currents from AAV2/1-*Cba*-eGFP–transduced wild-type hair cells after RWM injections at P0 to P2. Whole-cell, tight-seal recording revealed sensory transduction currents from eGFP-positive IHCs that were similar to those of GFP-negative control hair cells from the same tissue (Fig. 2, C **to** F) and similar to currents of uninjected control cells (11). The sensitivity of the cells, as indicated by the steepness of the stimulus-response relationship, was unaltered in the eGFP-positive cochlear hair cells relative to control cells (Fig. 2, D **to** F). Current amplitudes (Fig. 2E) and adaptation properties (Fig. 2C) were also unaffected, suggesting that viral transduction and eGFP expression do not alter sensory transduction. Because sensory transduction has not been previously recorded after the in vivo injection of viral vectors, these data offer assurance that hair cell function is not compromised by AAV2/1 injection or eGFP expression.

To assay for possible consequences of intracochlear injection of AAV2/1-*Cba*-eGFP on auditory function, we recorded auditory brain- stem responses (ABRs) from ears of injected and uninjected wild-type mice at P25 (Fig. 2G). The ABR assay uses scalp electrodes to

monitor the summed electrical activity of the auditory brainstem, with the first peak representing activity in the 8th cranial nerve. Consistent with previous studies that showed no detrimental effect on ABRs after in utero injection (18) or adult injection (19), auditory thresholds were not significantly different between uninjected wild-type control mice, wild-type mice that received a sham RWM injection with phosphate- buffered saline ($P = 0.27$, t test), or wild-type mice that received RWM injection that contained AAV2/1-*Cmv*-eGFP ($P = 0.95$, t test) (Fig. 2H). In summary, neither the injection technique, AAV transduction, nor eGFP expression affected hair cell or auditory function in any of our assays, suggesting that AAV2/1 vectors are safe for delivery of exogenous genes into the inner ears of neonatal mice.

AAV2/1-Cba-Tmc vectors rescue hair cell function in vitro

To assess the potential for gene therapy restoration of hair cell and auditory function, we generated AAV2/1-*Cba* vectors that carried the coding sequence for wild-type *Tmc1* or *Tmc2* fused to 3xFLAG tags at their C termini. To evaluate the functionality of these vectors, we applied the AAV2/1-*Cba-Tmc1* or AAV2/1-*Cba-Tmc2* vectors di- rectly to organotypic cochlear cultures excised at P0 from $Tmc1^{D/D};Tmc2^{D/D}$ mice, which lack TMC1 and TMC2 protein expression, are deaf, and lack sensory transduction in both OHCs (10) and IHCs (11). After 5 to 7 days, hair cells of the vector-exposed $Tmc1^{D/D};Tmc2^{D/D}$ cultures recovered FM1-43 uptake (fig. S3A), a styryl dye that permeates transduction channels open at rest (20–22). Because uninfected hair cells from $Tmc1^{D/D}$;$Tmc2^{D/D}$ do not take up FM1-43 (10), dye uptake in cells exposed to AAV2/1-*Cba-Tmc* vectors indicates recovery of sensory transduction.

Sensory transduction currents were recorded from both IHCs and OHCs. Figure S3B shows representative currents recorded from $Tmc1^{D/D}$;$Tmc2^{D/D}$ hair cells and hair cells in the same tissue 5 to 7 days after exposure to AAV2/1-*Cba-Tmc1*. Peak sensory transduction currents from OHCs ranged in amplitude from 66 to 420 pA, and those from IHCs ranged from 50 to 800 pA (Fig. S3B). The average (±SD) peak transduction current for IHCs rescued by AAV2/1-*Cba-Tmc1* was 306 ± 211 pA ($n = 4$), and that for OHCs, 289 ± 98 pA ($n = 10$). For IHCs rescued by AAV2/1-*Cba-Tmc2,* the mean peak transduction current was 766 ± 142 pA ($n = 2$). These results demonstrate that either *Tmc1* or *Tmc2* can restore sensory transduction at the cellular level when delivered into nonfunctional hair cells in vitro.

AAV2/1-Cba-Tmc vectors restore sensory transduction in vivo

To evaluate the ability of AAV2/1-*Cba-Tmc1* vectors to drive exogenous expression of *Tmc1* in vivo, we used quantitative reverse transcription polymerase chain reaction (RT-PCR) with primers specific for *Tmc1* mRNA (10). $Tmc1^{D/D}$ mice were injected at P1 with AAV2/1-*Cba-Tmc1* at a titer of 2×10^{13} gc/ml into one ear. RNA was harvested from injected and uninjected cochleas at P14. Injected cochleas had *Tmc1* mRNA expression levels that were 12-fold higher than those in uninjected cochleas (Fig. 3A), consistent with AAV2/1-*Cba-Tmc1*-driven expression of exogenous *Tmc1*.

To test the ability of the AAV-*Cba-Tmc* vectors to drive TMC protein expression in hair cells in vivo, we injected *Tmc1*$^{D/D}$;*Tmc2*$^{D/D}$ mice at P0 to P2 and excised cochlear tissue 6 to 7 days later. We observed prominent *Tmc1*-3xFLAG staining in the cell bodies of most IHCs (Fig. 3, B **and** C) and at the tips of IHC stereocilia (Fig. 3D), the site of hair cell sensory transduction, which confirmed that TMC1 and TMC2 were expressed and properly targeted. Consistent with our previous in vivo observation (Fig. 2 **and** Fig. S1), we saw little expression of the exogenous protein in OHCs (Fig. 3, B **to** D).

To assay for rescue of FM1-43 uptake and hair cell sensory transduction, live cochlea were excised at P6 to P7 and maintained in organotypic cultures until the equivalent of P8 to P9. FM1-43FX was pipetted over the tissue. Figure 3E shows a representative image of a cochlear culture harvested from a *Tmc1*$^{D/D}$;*Tmc2*$^{D/D}$ mouse exposed to FM1-43FX, which reveals no dye uptake in IHCs or OHCs. In contrast, *Tmc1*$^{D/D}$;*Tmc2*$^{D/D}$ mice injected with AAV2/1-*Cba-Tmc1* vectors had robust FM1-43FX uptake in most IHCs (71%, 57 of 80 cells) along the entire length of the cochlea in the injected ear (Fig. 3F). Very few OHCs took up the dye, consistent with a lack of viral transduction in OHCs in vivo.

Because FLAG and FM1-43 labeling indicated high viral transduction rates in IHCs in AAV2/1-*Cba-Tmc1*–injected cochleas, we assayed for rescue of sensory transduction current in cochlear IHCs at P7 to P9. Sensory transduction currents were recorded from AAV-*Cba-Tmc*-positive IHCs that expressed exogenous *Tmc1* or *Tmc2* (Fig. 3G), identified by the presence of FM1-43 uptake. Although the FM1-43 uptake data revealed variable viral transduction throughout the cochlea, cells that were FM1-43-positive had normal sensory transduction current amplitudes (Fig. 3, G **and** H) and normal sensitivity (Fig. 3, I **and** J), relative to wild-type (11) and GFP-positive controls (Fig. 2, C **to** F). FM1-43–negative cells from the same ear lacked sensory transduction currents entirely (Fig. 3, G **and** H). The differences in adaptation rate and extent between hair cells exposed to AAV2/1-*Cba-Tmc1* and AAV2/1-*Cba-Tmc2* (Fig. 3G) were consistent with the differences observed in hair cells expressing endogenous *Tmc1* or *Tmc2* (11). In summary, the single hair cell physiology data suggest that AAV2/1-*Cba-Tmc* vectors are capable of complete restoration of sensory transduction in vivo with all the properties of native sensory transduction.

AAV2/1-Cba-Tmc1 rescues ABRs in Tmc1-deficient mice

To model AAV gene therapy for rescue of genetic deafness in patients who carry recessive mutations in *Tmc1*, we injected *Tmc1*-deficient animals (P0 to P2) in vivo with AAV2/1-*Cba-Tmc1* and measured the auditory function at 25 to 30 days. Figure 4A shows families of ABR waveforms recorded in response to 8-kHz tone bursts. The data were recorded from an uninjected *Tmc1*$^{D/D}$ mouse and a *Tmc1*$^{D/D}$ mouse injected with AAV2/1-*Cba-Tmc1*. Uninjected *Tmc1*$^{D/D}$ mice lacked responses at all stimulus intensities and frequencies tested, which ranged between 0 and 115 dB and 5 and 32 kHz, respectively, indicating profound deafness, consistent with previous reports (9). However, prominent ABR waveforms, which represented substantial recovery of auditory transmission from the cochlea to the brainstem via the 8th cranial nerve, were present in 50% (8 of 16) of the AAV2/1-*Cba-Tmc1*-injected mice. In the eight mice with no recovery of ABR responses, we found little evidence of viral

transduction in hair cells, suggesting that the injections may have been unsuccessful, perhaps due to clogged or improperly targeted injection needles.

For the eight AAV2/1-*Cba-Tmc1*-injected mice with auditory responses, we quantified peak 1 amplitudes as a function of stimulus intensity at 8 kHz and compared them with those observed in uninjected *Tmc1*$^{D/D}$ control mice (Fig. 4B). Peak 1 amplitudes increased monotonically in the eight *Tmc1*$^{D/D}$ mice injected with AAV-*Cba-Tmc1*, indicating a stimulus-dependent increase in the auditory response. Minimum ABR thresholds showed recovery of auditory function in these mice, particularly at frequencies between 5 and 16 kHz (Fig. 4C). The ABR thresholds at 85 to 100 dB (Fig. 4C) represent a substantial improvement relative to uninjected *Tmc1*$^{D/D}$ control mice, which are profoundly deaf and have no detectable responses to sound stimuli even at 115 dB, the highest intensity tested. The data demonstrate partial recovery of auditory function at the systems level in the otherwise deaf mice.

Although there was recovery of ABR responses in the AAV2/1-*Cba-Tmc1*-injected mice, the responses did not reach wild-type levels (Fig. 2H). To investigate the reason for the incomplete recovery, including possible toxicity associated with overexpression of *Tmc1*, we injected wild-type C57BL/6 mice with AAV2/1-*Cba-Tmc1*. ABR thresholds in the AAV2/1-*Cba-Tmc1*-injected wild-type mice were unaltered relative to uninjected controls (Fig. S4A). This finding suggests that there is little toxicity associated with the injection procedure, exposure to AAV2/1-*Cba-Tmc1* vectors, or overexpression of *Tmc1* in hair cells, spiral ganglion neurons, or any other cell type necessary for normal auditory function. Furthermore, we did not observe FM1-43 uptake in non-hair cells (Fig. 3, E **and** F), suggesting that aberrant expression of *Tmc1* does not lead to the formation of functional channels in other cell types.

To investigate other possible causes of the incomplete recovery, we measured distortion product otoacoustic emissions (DPOAEs) in uninjected *Tmc1*$^{D/D}$ mice and *Tmc1*$^{D/D}$ mice injected with AAV2/1-*Cba- Tmc1.* The DPOAE assay is a specific test for OHC function. OHCs are required for cochlear amplification, enhanced sensitivity, and normal auditory function (23, 24). DPOAE measurements revealed elevated thresholds relative to wild-type mice and no difference between uninjected *Tmc1*$^{D/D}$ mice and those injected with AAV2/1-*Cba-Tmc1* vectors (Fig. 4D), which suggests little recovery of OHC function. Uninjected wild-type mice and wild-type mice injected with either AAV2/1-*Cba*-eGFP or AAV2/1-*Cba-Tmc1* had normal DPOAE thresholds (Fig. S4B), consistent with the suggestion that the injection itself, exposure to AAV2/1 vectors, and *Tmc1* overexpression caused little toxicity in OHCs or elsewhere in the cochlea.

After the ABR and DPOAE measurements, the mice were euthanized and their inner ear tissue was excised for histological examination. There was no overt evidence of inflammation, tissue damage, or decay in the injected ears. Cochlear whole mounts were stained with an anti-MYO7A antibody to label hair cells and with Alexa546-phalloidin to label hair bundles (Fig. 4F). Counts of surviving IHCs revealed no significant difference (P = 0.6) between uninjected *Tmc1*$^{D/D}$ cochleas and those injected with AAV2/1-*Cba-Tmc1* (Fig. 4E), suggesting that AAV2/1-*Cba-Tmc1* injection was neither detrimental nor

beneficial for IHC survival at P30. Hair bundle morphology and tip links remain normal in surviving *Tmc1*$^{D/D}$ hair cells (10), and we detected no changes after AAV2/1-*Cba-Tmc1* injection.

AAV2/1-Cba-Tmc2 restores ABRs in Tmc1 mutant mice

Tmc2, a closely related ortholog of *Tmc1,* is expressed in cochlear hair cells during the first postnatal week, but mRNA levels decline thereafter (10). *Tmc2* is expressed in *Tmc1*$^{D/D}$ mice, and both IHCs and OHCs in these mice retain sensory transduction through the end of the first postnatal week (10, 11). However, because *Tmc2* expression declines thereafter, *Tmc1*$^{D/D}$ mice are deaf. AAV2/1-*Cba-Tmc2* restored sensory transduction in *Tmc1*$^{D/D}$;*Tmc2*$^{D/D}$ hair cells in vitro and in vivo (Fig. 3, G **and** H); therefore, we investigated whether AAV2/1-*Cba- Tmc2* injection into the ears of *Tmc1*$^{D/D}$ mice would also restore auditory function. To test this possibility, we used the same injection protocols (as AAV2/1-*Cba-Tmc1*) and measured ABR responses at P25 to P30. We recorded prominent ABR responses in 9 of 16 *Tmc1*$^{D/D}$ mice injected with AAV2/1-*Cba-Tmc2* (Fig. 5A). Peak 1 amplitudes (Fig. 5B) and minimal ABR thresholds (Fig. 5C) were similar to those of mice injected with AAV2/1-*Cba-Tmc1* (Fig. 4, B **and** C), suggesting that expression of exogenous *Tmc2* is capable of restoring auditory function in vivo. Also similar to AAV2/1-*Cba-Tmc1*, AAV2/1-*Cba-Tmc2* injection did not restore DPOAE thresholds (Fig. S4B), nor did it affect hair cell survival or death rates relative to uninjected *Tmc1*$^{D/D}$ control mice (Fig. 5D **and** Fig. S5). There was no significant difference ($P = 0.44$) in IHC counts between uninjected *Tmc1*$^{D/D}$ mice and those injected with AAV2/1-*Cba-Tmc2* (Fig. 5E).

On the basis of the ability of exogenous *Tmc2* to restore ABR responses in mouse models of genetic deafness due to recessive *TMC1* mutations, we next asked whether exogenous *Tmc2* expression might be sufficient to overcome dominant *TMC1* mutations and restore auditory function. Previously, Pan *et al.* (11) showed that the dominant p.M412K mutation in TMC1, known as *Bth*, causes a reduction in calcium permeability, a reduction in single-channel currents, and an increase in the number of sensory transduction channels in IHCs. The identical mutation has also recently been described in a human family in the orthologous residue of human TMC1 p.M418K (15), suggesting that the *Bth* mouse is an ideal model for genetic hearing loss in humans. To investigate the ability of *Tmc2* to compensate for the *Tmc1-Bth* mutation, we injected AAV2/1-*Cba-Tmc2* vectors into the ears of homozygous *Bth* mice and measured their ABRs at P25 to P30. Consistent with previous reports, *Bth* mice were completely deaf by P15 (13, 14). However, 7 of 15 *Bth* mice injected with AAV2/1-*Cba- Tmc2* had prominent ABRs evoked by loud sound intensities (Fig. 6A). Peak 1 amplitudes were smaller and the thresholds were elevated (Fig. 6, B **and** C) relative to ABRs evoked in *Tmc1*$^{D/D}$ mice injected with either AAV2/1-*Cba-Tmc2* (Fig. 5, B **and** C) or AAV2/1-*Cba-Tmc1* (Fig. 4, B **and** C), suggesting that the extent of the recovery was limited. There was a significant increase in the survival rate of IHCs in the ears of *Bth* mice injected with AAV2/1-*Cba-Tmc2* relative to the uninjected ears (Fig. 6, D **and** E, **and** Fig. S6), suggesting that exogenous expression of *Tmc2* promotes IHC survival.

AAV2/1-Cba-Tmc vectors restore behavioral responses to auditory stimuli

Partial ABR recovery in deaf mice injected with AAV2/1-*Cba-Tmc* vectors may have resulted in behaviorally relevant sound perception. We therefore tested acoustic startle reflexes at P30 from wild-type control mice, uninjected deaf mice, and deaf mice injected with AAV2/1-*Cba-Tmc* vectors. Wild-type mice had startle responses that were detectable beginning around 80 dB (Fig. 7A), whereas *Tmc1*$^{D/D}$ deaf mice lacked startle responses at all frequencies and sound intensities tested (Fig. 7B). When we measured acoustic startle responses in five *Tmc1*$^{D/D}$ mice injected with AAV2/1-*Cba-Tmc1* that lacked ABR responses, we found that they also lacked startle responses (Fig. 7A, **open squares**), perhaps due to failed injections. However, we found that 100% (n = 7) of *Tmc1*$^{D/D}$ mice injected with AAV2/1-*Cba-Tmc1* that had ABR responses also had robust startle responses (Fig. 7A). All seven mice had recovery of startle response thresholds at 90 to 100 dB with startle amplitudes that increased with increasing sound intensity. Furthermore, we found that the startle responses were also present at P60, the latest time point tested: five of five *Tmc1*$^{D/D}$ mice injected with AAV2/1-*Cba-Tmc1* that had positive ABRs also had substantial startle responses (Fig. 7B).

Next, we examined startle responses in *Tmc1* mutant mice injected with AAV2/1-*Cba-Tmc2.* Although five *Tmc1*$^{D/D}$ mice injected with AAV2/1-*Cba-Tmc2* recovered ABRs and were tested for startle responses, only two of the five had startle responses (Fig. 7C). One mouse had substantial responses, similar to those of wild-type mice for the loudest sound intensities (Fig. 7C). Seven of 15 *Tmc1*^{Bth} mice injected with AAV2/1-*Cba-Tmc2* recovered ABR responses, but none had startle responses (Fig. 7, C **and** D), suggesting that exogenous *Tmc2* expression may not be sufficient to overcome the dominant *Bth* mutation in a behaviorally relevant assay.

Figure 7D summarizes the ABR and startle response data for all 55 *Tmc1* mutant mice injected with AAV2/1-*Cba-Tmc* vectors. Gene augmentation with wild-type *Tmc1* successfully restored both ABR and acoustic startle responses in more than 50% of the injected *Tmc1*$^{D/D}$ mice. Injection of the AAV2/1 vector encoding wild-type *Tmc2* revealed similar success rates for ABR recovery, but was less effective for the recovery of startle responses in both *Tmc1*$^{D/D}$ and *Tmc1*^{Bth} mice.

Discussion

To model gene therapy for DFNB7/11, we used mice deficient in *Tmc1* and engineered AAV2/1 vectors that carried the *Cba* promoter and the coding sequence for either *Tmc1* or *Tmc2*. Viral transduction with either AAV2/1-*Cba-Tmc1* or AAV2/1-*Cba-Tmc2* revealed localization of exogenous TMC1 and TMC2 at the tips of hair cell stereocilia, uptake of the transduction channel permeable dye FM1-43, and robust mechanosensory transduction currents in otherwise nonfunctional hair cells. The data provide compelling evidence that the vectors can restore function at the cellular level in vitro.

In vivo injection, via the RWM, of either AAV2/1-*Cmv*-eGFP or AAV2/1-*Cba*-eGFP drove robust expression of eGFP in cochlear and vestibular hair cells, suggesting that the approach may be viable for the delivery of therapeutic reagents to target hair cells throughout the

human inner ear. Normal mechanosensory responses and normal ABRs suggested that the injection technique, AAV2/1 vectors, and eGFP expression are safe for in vivo use, supporting further development of AAV gene therapy as a strategy for hearing restoration. Consistent with previous observations (5), when AAV2/1 vectors were injected via the RWM into the inner ears of deaf mice, restoration of cellular function was limited to IHCs. We found little evidence of exogenous gene expression in OHCs after injection of four different vectors. Because all vectors were capable of driving exogenous gene expression in OHCs in vitro, we suspect that the lack of viral transduction in OHCs in vivo resulted from limited viral access to the hair cell apical surface via RWM injection into perilymphatic spaces. Kilpatrick *et al.* (19) reported that introduction of AAV vectors into the scala media, which bathes hair cell apical membranes, yielded GFP expression in both IHCs and OHCs. The challenge of scala media injection is that it requires a more invasive surgical approach and can cause mixing of high K^+ (~140 mM) endolymph and perilymph leading to hair cell de- polarization and cell death. To target OHCs may require vectors that can enter via the basolateral membrane or delivery methods that target endolymphatic spaces without disrupting endolymph/perilymph barriers.

ABRs were recovered in >50% of *Tmc1*$^{D/D}$ deaf mice injected with AAV2/1-*Cba-Tmc1*, indicating successful transmission of auditory information from the cochlea to the auditory brainstem. The ABR thresholds were elevated relative to those of wildtype mice, indicating incomplete recovery of auditory function. DPOAE responses did not recover, suggesting that the elevated ABR thresholds were due to lack of recovery of OHC function, in turn due to low viral transduction rates in OHCs. Functional OHCs are required for cochlear amplification, a process that provides mechanical feedback to the cochlea by increasing gain to soft sounds. OHC dysfunction is known to yield elevated ABR thresholds, shifted up to 60 dB higher than wild type. Thus, in *Tmc1*$^{D/D}$ mice, in which all cochlear hair cells lack sensory transduction, rescue of IHC but not OHC function yielded ABR thresholds ~60 dB higher than wild type, similar to thresholds in mice with OHC dysfunction (24). In *Vglut3* knockout mice, OHCs remain functional but the mice are deaf because of IHC dysfunction (5). After *Vglut3* gene augmentation, ABR thresholds recovered to near wild-type levels because restoration of function was only required in IHCs, which account for ~25% of the cochlear hair cell population. Our experiments revealed high viral transduction rates in IHCs and the transduced cells had mechanosensory currents equivalent to those of wild type, but the OHC dysfunction remained. Although the recovery was incomplete, the result was considered a success because normal mechanosensory function in IHCs is a prerequisite for auditory function. Had the outcome been the converse—restoration of OHC but not IHC function—the animals would still be deaf.

We also found that AAV2/1-*Cba-Tmc2* vectors were capable of restoring sensory transduction and partial ABR responses in *Tmc1*$^{D/D}$ mice, which supports the hypothesis that *Tmc1* and *Tmc2* perform somewhat redundant functions and can substitute for each other, at least in IHCs. The AAV2/1-*Cba-Tmc2* transduction pattern was similar to AAV2/1-*Cba-Tmc1* and was restricted primarily to IHCs, resulting in similar recovery at elevated ABR thresholds. That hair cell survival rates were not altered in *Tmc1*$^{D/D}$ mice injected with either AAV2/1-*Cba-Tmc1* or AAV2/1-*Cba-Tmc2* was important for two reasons: (i) neither vector caused loss or decay of hair cells, and (ii) hair cells remained in uninjected *Tmc1*$^{D/D}$

mice up to P60, suggesting that there may be a window of opportunity for therapeutic intervention. Whether a similar window exists in humans with recessive *TMC1* mutations is unknown. If patients with *TMC1* mutations retain viable hair cells, they may present an opportunity for clinical intervention.

Restoration of auditory function was limited in *Bth* mice injected with AAV2/1-*Cba-Tmc2*. There was significant preservation of IHCs in AAV2/1-*Cba-Tmc2*–injected *Bth* mice. The mechanism that promoted IHC survival is unknown. On the basis of the measurements of sensory transduction and calcium permeability in mice that expressed wild-type *Tmc2*, *Tmc1*, or *Tmc1-Bth*, Pan *et al.* (11) found a significant reduction in calcium entry in *Tmc1-Bth* IHCs, whereas *Tmc2* cells had high calcium entry. We hypothesize that appropriate levels of calcium entry are required for maintenance and survival of IHCs. Therefore, by introducing exogenous *Tmc2,* calcium homeostasis was restored, which enhanced hair cell survival in the *Bth* mice injected with AAV2/1-*Cba-Tmc2.*

As a final test of auditory function, we measured acoustic startle reflexes in *Tmc1* mutant mice. The otherwise unresponsive $Tmc1^{D/D}$ mice recovered startle responses after injection of AAV2/1-*Cba-Tmc1*, and the responses persisted for up to 60 days, the latest time point tested. It was unclear why *Tmc1-Bth* mice injected with AAV2/1-*Cba- Tmc2* recovered partial ABR function but did not recover startle responses. The extent of the ABR recovery in *Tmc1-Bth* mice injected with AAV2/1-*Cba-Tmc2* was less than the ABR recovery in $Tmc1^{D/D}$ mice injected with AAV2/1-*Cba-Tmc2,* suggesting that there may be a minimal threshold required to drive behavioral responses to loud sounds. Therapies aimed at restoration of auditory function for dominant DFNA36 deafness may require development of alternate strategies, perhaps by suppression of the dominant allele.

In conclusion, the data provide compelling proof-of-principle evidence demonstrating that gene augmentation in a mouse model of DFNB7/11 is effective in restoring cellular function in vitro in both IHCs and OHCs, restoring IHC function in vivo, partial recovery of systems level function in vivo, and recovery of acoustic startle reflexes at the behavioral level. Recovery of ABR and startle responses was likely a direct result of recovery of IHC sensory transduction at the cellular level and suggests that *Tmc1* re-expression can restore auditory function at every level.

Thirty-five *TMC1* mutations have been identified that cause recessive prelingual deafness in humans, which underscores the significance of TMC1 for normal auditory function and the need for therapeutic reagents to remedy the disorder. Although our gene therapy strategy is not yet ready for clinical application, the challenges that remain are not insurmountable. Continued development of *Tmc* gene therapy will need to provide characterization of the long-term expression pattern of the exogenous constructs, including their ability to maintain recovery; improved design of vectors, promoters, and delivery techniques that drive exogenous gene expression in OHCs; and further evaluation of the therapeutic window of opportunity in humans with recessive *TMC1* mutations. Finally, we suggest that AAV-mediated gene augmentation in the inner ear may be a model that could be expanded to address some of the more than 70 forms of genetic deafness.

Materials and Methods

Study design

The aim of this study was to identify AAV serotypes and promoters for delivery and expression of exogenous *Tmc1* and *Tmc2* in hair cells of the mouse cochlea and to evaluate the ability of these vectors to restore function in mouse models of genetic deafness in humans. AAV vectors were injected in vivo, and the outcomes were evaluated using quantitative RT-PCR, immunolocalization and confocal microscopy, imaging FM1-43 uptake, single-cell recording, histology and imaging of whole cochleas, measurement of ABRs, DPOAEs, and acoustic startle reflexes. Left ears were injected and right ears were used as uninjected controls. Each experiment was replicated as indicated by n values in the figure legends. All experiments with mice and viral vectors were approved by the Institutional Animal Care and Use Committee (protocols #2146 and #2878) at Boston Children's Hospital and the Institutional Biosafety Committee (protocol #IBC-P00000447).

In vivo injection of viral vectors

Mouse pups (P0 to P2) were injected via the RWM using beveled glass microinjection pipettes, as described in Supplementary Methods.

Hair cell electrophysiology

Organotypic cochlear cultures were bathed in standard artificial perilymph containing 137 mM NaCl, 0.7 mM NaH_2PO_4, 5.8 mM KCl, 1.3 mM $CaCl_2$, 0.9 mM $MgCl_2$, 10 mM Hepes, and 5.6 mM $_D$-glucose. Vitamins (1:50) and amino acids (1:100) were added to the solution from concentrates (Invitrogen), and NaOH was used to adjust the fi- nal pH to 7.40 (310 mosmol/kg). Recording pipettes (3 to 5 megohms) were pulled from R6 capillary glass (King Precision Glass) and filled with intracellular solution containing 135 mM CsCl, 5 mM Hepes, 5 mM EGTA, 2.5 mM $MgCl_2$, 2.5 mM Na_2–adenosine triphosphate, and 0.1 mM $CaCl_2$, where CsOH was used to adjust the final pH to (285 mosmol/kg). Whole-cell, tight-seal voltage-clamp recordings were done at −84 mV at room temperature (22° to 24°C) using an Axopatch 200B amplifier (Molecular Devices). Sensory transduction currents were filtered at 10 kHz with a low-pass Bessel filter and digitized at ≥20 kHz with a 16-bit acquisition board (Digidata 1440A) and pCLAMP 10 software (Molecular Devices). Data were stored for off- line analysis using OriginPro 8 (OriginLab).

ABR and DPOAE

ABR recordings were conducted as described previously (25), at 32°C in a soundproof chamber. To test hearing function, anesthetized mice were presented pure tone stimuli of 5.6, 8, 11.3, 16, 22.6, or 32 kHz at sound pressure levels between 10 and 115 dB in 5-dB steps until a threshold intensity that evoked a reproducible ABR waveform (peaks 1 to 4) was detected. Responses were collected, and data were analyzed as described in Supplementary Methods.

DPOAE data were collected under the same conditions and during the same recording sessions as the ABR data. Primary tones were produced at a frequency ratio of 1.2 (f_2/f_1) for the generation of DPOAEs at $2f_1–f_2$, where the f_2 level was 10 dB sound pressure level

below f_1 level for each f_2/f_1 pair. The f_2 levels were swept in 5-dB steps from 20 to 80 dB. Waveform and spectral analyses are described in Supplementary Methods.

Acoustic startle reflexes

Mice were tested for startle reflexes in response to broadband auditory stimulation at varying intensities, as described in Supplementary Methods.

Statistical analysis

All mean values and error bars presented in the figures represent mean ± SD. Comparisons for statistical significance between injected ears and uninjected ears were performed using a two-tailed paired *t* test. $P < 0.05$ was considered significant.

Supplementary Material

Refer to Web version on PubMed Central for supplementary material.

Acknowledgments:

We thank M. C. Liberman for assistance with ABR recordings; Y. Shu and Z.-Y. Chen for technical assistance with RWM injections; V. Padrun, F. Pidoux, and A. Aebi at École Polytechnique Fédérale de Lausanne (EPFL) Brain Mind Institute for technical assistance with AAV production; Behavior and Viral Cores at Boston Children's Hospital [supported by Boston Children's Hospital Intellectual and Developmental Disabilities Research Center (BCH IDDRC), P30 HD18655]. Funding: This work was supported by the Bertarelli Foundation, Program in Translational Neuroscience and Neuroengineering, Kidz b Kidz Foundation and Jessica and David Freier.

References

1. Géléoc GSG, Holt JR, Sound strategies for hearing restoration. Science 344, 1241062 (2014). [PubMed: 24812404]
2. Kohrman DC, Raphael Y, Gene therapy for deafness. Gene Ther. 20, 1119–1123 (2013). [PubMed: 23864018]
3. Kesser BW, Hashisaki GT, Fletcher K, Eppard H, Holt JR, An *in vitro* model system to study gene therapy in the human inner ear. Gene Ther. 14, 1121–1131 (2007). [PubMed: 17568767]
4. Kesser BW, Hashisaki GT, Holt JR, Gene transfer in human vestibular epithelia and the prospects for inner ear gene therapy. Laryngoscope 118, 821–831 (2008). [PubMed: 18300702]
5. Akil O, Seal RP, Burke K, Wang C, Alemi A, During M, Edwards RH, Lustig LR, Restoration of hearing in the VGLUT3 knockout mouse using virally mediated gene therapy. Neuron 75, 283–293 (2012). [PubMed: 22841313]
6. Kitajiri S-I, McNamara R, Makishima T, Husnain T, Zafar AU, Kittles RA, Ahmed ZM, Friedman TB, Riazuddin S, Griffith AJ, Identities, frequencies and origins of TMC1 mutations causing DFNB7/B11 deafness in Pakistan. Clin. Genet. 72, 546–550 (2007). [PubMed: 17877751]
7. Sirmaci A, Duman D, Öztürkmen-Akay H, Erbek S, İncesulu A, Öztürk-Hişmi B, Arici ZS, Yüksel-Konuk EB, Taşir-Yilmaz S, Tokgöz-Yilmaz S, Cengiz FB, Aslan İ, Yildirim M, Hasanefendioğlu-Bayrak, Ayçiçek A, Yilmaz İ, Fitoz S, Altin F, Özdağ H, Tekin M, Mutations in *TMC1* contribute significantly to nonsyndromic autosomal recessive sensori- neural hearing loss: A report of five novel mutations. Int. J. Pediatr. Otorhinolaryngol. 73, 699–705 (2009). [PubMed: 19187973]
8. Kawashima Y, Kurima K, Pan B, Griffith AJ, Holt JR, Transmembrane channel-like (TMC) genes are required for auditory and vestibular mechanosensation. Pflugers Arch. 467, 85–94 (2015). [PubMed: 25074487]
9. Nakanishi H, Kurima K, Kawashima Y, Griffith AJ, Mutations of TMC1 cause deafness by disrupting mechanoelectrical transduction. Auris Nasus Larynx 41, 399–408 (2014). [PubMed: 24933710]

10. Kawashima Y, Géléoc GSG, Kurima K, Labay V, Lelli A, Asai Y, Makishima T, Wu DK, Della Santina CC, Holt JR, Griffith AJ, Mechanotransduction in mouse inner ear hair cells requires transmembrane channel-like genes. J. Clin. Invest. 121, 4796–4809 (2011). [PubMed: 22105175]
11. Pan B, Géléoc GSG, Asai Y, Horwitz GC, Kurima K, Ishikawa K, Kawashima Y, Griffith AJ, Holt JR, TMC1 and TMC2 are components of the mechanotransduction channel in hair cells of the mammalian inner ear. Neuron 79, 504–515 (2013). [PubMed: 23871232]
12. Beurg M, Xiong W, Zhao B, Müller U, Fettiplace R, Subunit determination of the conductance of hair-cell mechanotransducer channels. Proc. Natl. Acad. Sci. U.S.A. 112, 1589–1594 (2015). [PubMed: 25550511]
13. Marcotti W, Erven A, Johnson SL, Steel KP, Kros CJ, *Tmc1* is necessary for normal functional maturation and survival of inner and outer hair cells in the mouse cochlea. J. Physiol. 574, 677–698 (2006). [PubMed: 16627570]
14. Vreugde S, Erven A, Kros CJ, Marcotti W, Fuchs H, Kurima K, Wilcox ER, Friedman TB, Griffith AJ, Balling R, Hrabé De Angelis M, Avraham KB, Steel KP, Beethoven, a mouse model for dominant, progressive hearing loss DFNA36. Nat. Genet. 30, 257–258 (2002). [PubMed: 11850623]
15. Zhao Y, Wang D, Zong L, Zhao F, Guan L, Zhang P, Shi W, Lan L, Wang H, Li Q, Han B, Yang L, Jin X, Wang J, Wang J, Wang Q, A novel DFNA36 mutation in TMC1 orthologous to the Beethoven (Bth) mouse associated with autosomal dominant hearing loss in a Chinese family. PLOS One 9, e97064 (2014). [PubMed: 24827932]
16. Hernandez VH, Gehrt A, Reuter K, Jing Z, Jeschke M, Mendoza Schulz A, Hoch G, Bartels M, Vogt G, Garnham CW, Yawo H, Fukazawa Y, Augustine GJ, Bamberg E, Kügler S, Salditt T, de Hoz L, Strenzke N, Moser T, Optogenetic stimulation of the auditory pathway. J. Clin. Invest. 124, 1114–1129 (2014). [PubMed: 24509078]
17. Safieddine S, Wenthold RJ, SNARE complex at the ribbon synapses of cochlear hair cells: Analysis of synaptic vesicle- and synaptic membrane-associated proteins. Eur. J. Neurosci. 11, 803–812 (1999). [PubMed: 10103074]
18. Bedrosian JC, Gratton MA, Brigande JV, Tang W, Landau J, Bennett J, *In vivo* delivery of recombinant viruses to the fetal murine cochlea: Transduction characteristics and long- term effects on auditory function. Mol. Ther. 14, 328–335 (2006). [PubMed: 16765094]
19. Kilpatrick LA, Li Q, Yang J, Goddard JC, Fekete DM, Lang H, Adeno-associated virus-mediated gene delivery into the scala media of the normal and deafened adult mouse ear. Gene Ther. 18, 569–578 (2011). [PubMed: 21209625]
20. Gale JE, Marcotti W, Kennedy HJ, Kros CJ, Richardson GP, FM1–43 dye behaves as a per- meant blocker of the hair-cell mechanotransducer channel. J. Neurosci. 21, 7013–7025 (2001). [PubMed: 11549711]
21. Meyers JR, MacDonald RB, Duggan A, Lenzi D, Standaert DG, Corwin JT, Corey DP, Lighting up the senses: FM1–43 loading of sensory cells through nonselective ion channels. J. Neurosci. 23, 4054–4065 (2003). [PubMed: 12764092]
22. Géléoc GS, Holt JR, Developmental acquisition of sensory transduction in hair cells of the mouse inner ear. Nat. Neurosci. 10, 1019–1020 (2003).
23. Hudspeth AJ, Integrating the active process of hair cells with cochlear function. Nat. Rev. Neurosci. 15, 600–614 (2014). [PubMed: 25096182]
24. Liberman MC, Gao J, He DZZ, Wu X, Jia S, Zuo J, Prestin is required for electromotility of the outer hair cell and for the cochlear amplifier. Nature 419, 300–304 (2002). [PubMed: 12239568]
25. Maison SF, Liu X-P, Vetter DE, Eatock RA, Nathanson NM, Wess J, Liberman MC, Muscarinic signaling in the cochlea: Presynaptic and postsynaptic effects on efferent feedback and afferent excitability. J. Neurosci. 30, 6751–6762 (2010). [PubMed: 20463237]
26. Grimm D, Kay MA, Kleinschmidt JA, Helper virus-free, optically controllable, and two- plasmid-based production of adeno-associated virus vectors of serotypes 1 to 6. Mol. Ther. 7, 839–850 (2003). [PubMed: 12788658]
27. Stauffer AE, Holt JR, Sensory transduction and adaptation in inner and outer hair cells of the mouse auditory system. J. Neurophysiol. 98, 3360–3369 (2007). [PubMed: 17942617]

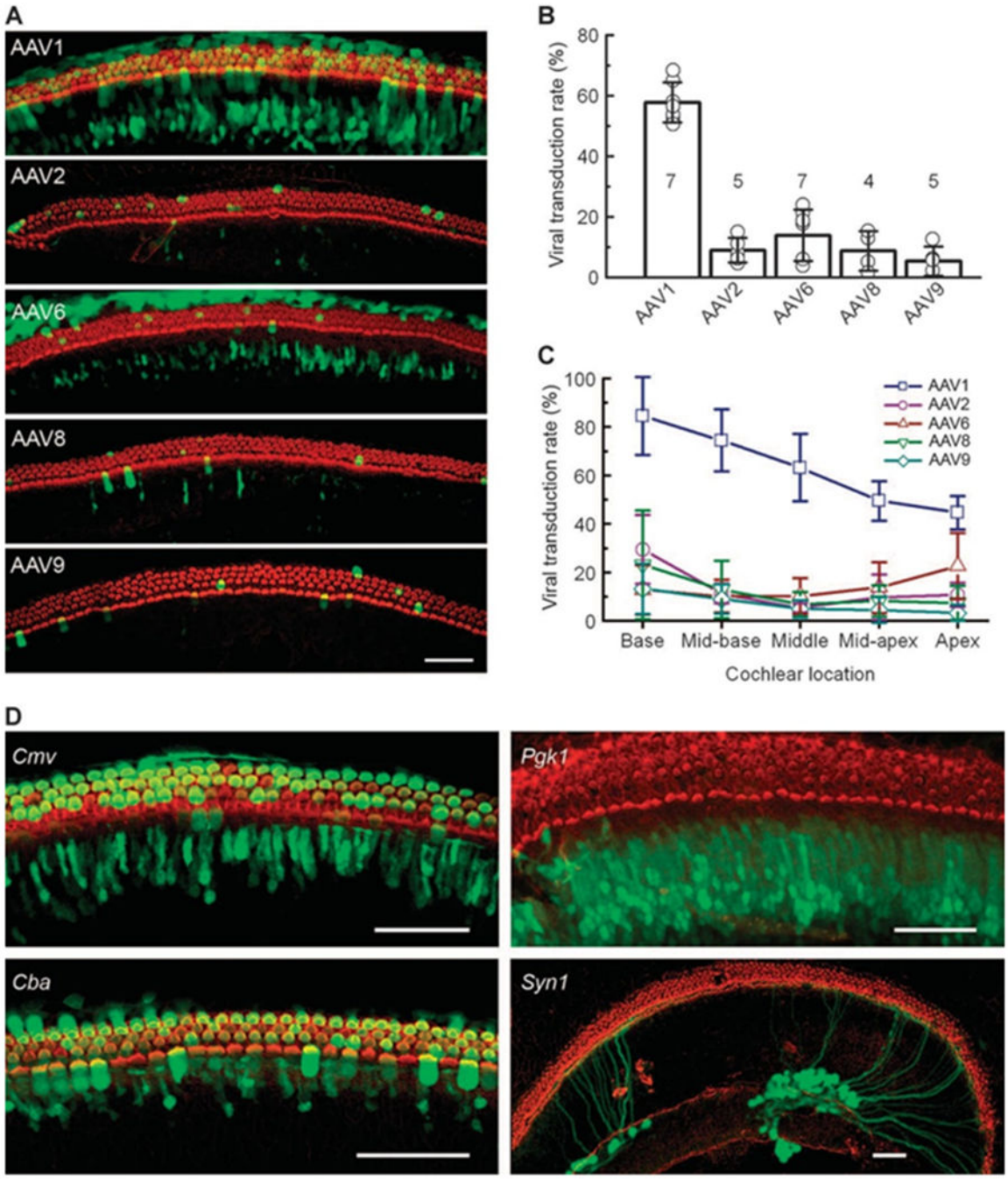

Figure 1: Screen for AAV serotype and promoter in cochlear hair cells.

(A) Representative confocal images of the mid-base of cochlear cultures exposed to AAV-*Cmv*-eGFP with capsid serotypes indicated. Wild-type (WT) cochleas were dissected at P0 and exposed to viral concentrations of 3.3×10^{10} gc/ml (AAV2/1, AAV2/2, and AAV2/6) or 3.3×10^{11} gc/ml (AAV2/8 and AAV2/9) for 24 hours. The tissue was cultured for 7 days, fixed, stained with Alexa 546–phalloidin (red) and imaged for GFP (green) on a Zeiss 700 confocal microscope. Projection images were generated from stacks of 20 to 40 optical sections collected at 1.2-mm intervals. Scale bar, 50 mm. (B) Viral transduction rates were

determined from the number of eGFP-positive hair cells (green) in each cochlea divided by the total hair cells with Alexa 546-phalloidin-positive hair bundles. Data are means ± SD (*n*, number of cochleas). Symbols show transduction rates for each cochlea. (C) Viral transduction rates for all hair cells subdivided into five equal regions and plotted for the entire length of the tonotopic axis. Data are means ± SD [*n* as shown in (B)]. (D) Representative images of cochleas dissected from P0 WT mice, exposed to AAV2/1-eGFP vectors with promoters indicated (titers: 1×10^{11} to 1×10^{12} gc/ml). Scale bars, 50 mm.

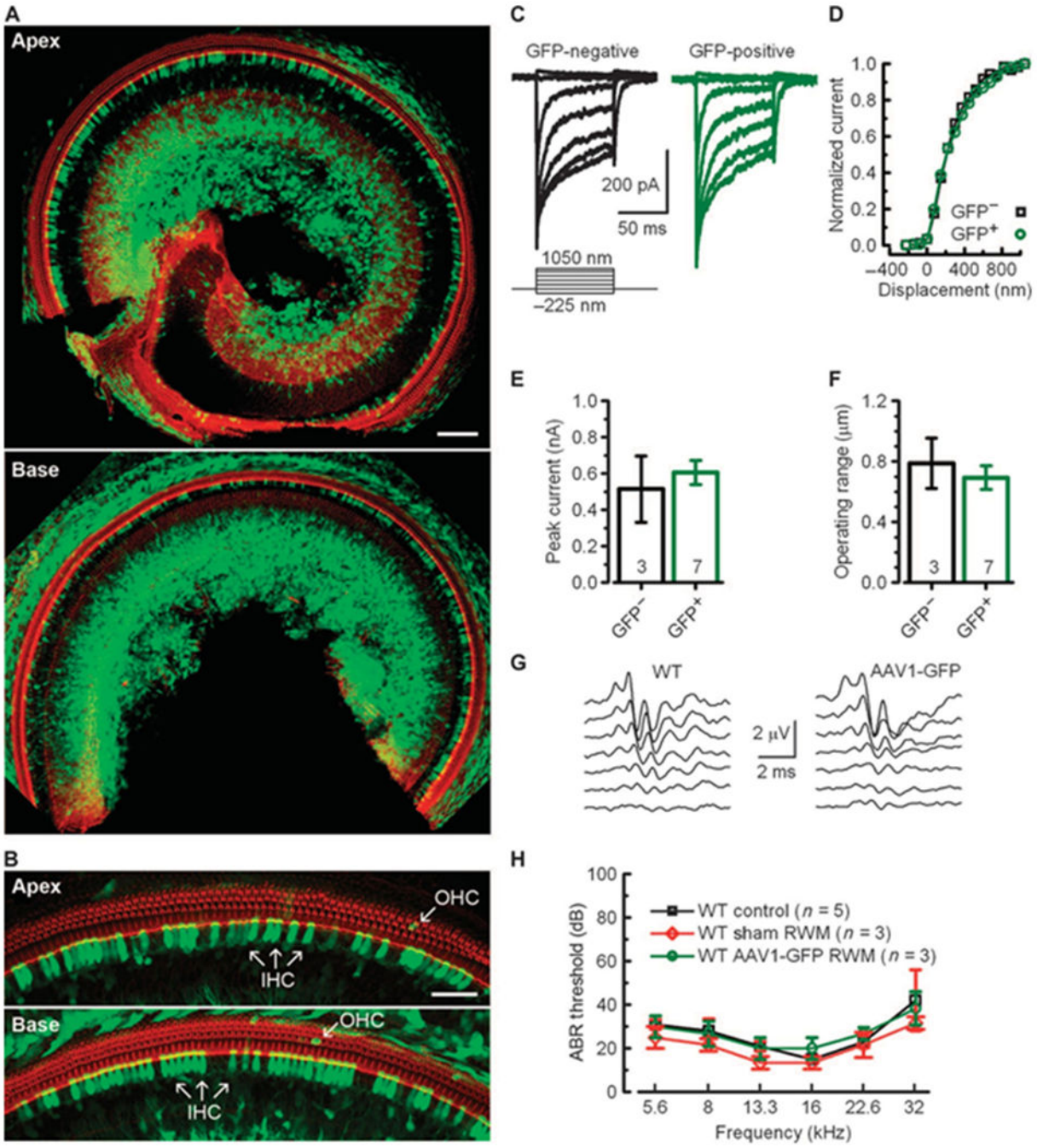

Figure 2: In vivo injection of AAV2/1-*Cba*-eGFP through the RWM.

(A) Representative confocal images from the apex and base of a WT cochlea injected through the RWM with 1 ml of AAV2/1-*Cba*-eGFP (6×10^{12} gc/ml) at P2, harvested at P9, and stained with Alexa 546–phalloidin (red) and imaged for GFP (green). Scale bar, 100 mm. (B) Apex and base from the same cochlea in (A) at higher magnification. Scale bar, 50 mm. (C) Families of sensory transduction currents evoked by mechanical displacement of IHC bundles from control (GFP-negative) cells and GFP-positive cells. Scale bars and displacement protocols are provided. (D) Stimulus-response curves for GFP-negative and

GFP-positive cells revealed no difference in sensitivity. (E and F) Peak sensory transduction currents (E) and 10 to 90% operating range (F) from control and GFP-positive cells. Data are means ± SD (*n*, number of cells). (G) Families of ABR waveforms recorded at P25 from uninjected WT and AAV2/1-*Cba*-eGFP injected ears. The stimulus was an 8-kHz tone burst between 25 and 70 dB in 5-dB increments. (H) Auditory thresholds plotted as a function of stimulus frequency for uninjected WT mice, sham-injected WT mice, and AAV2/1-*Cba*-eGFP-injected mice. Data are means ± SD (*n*, number of mice).

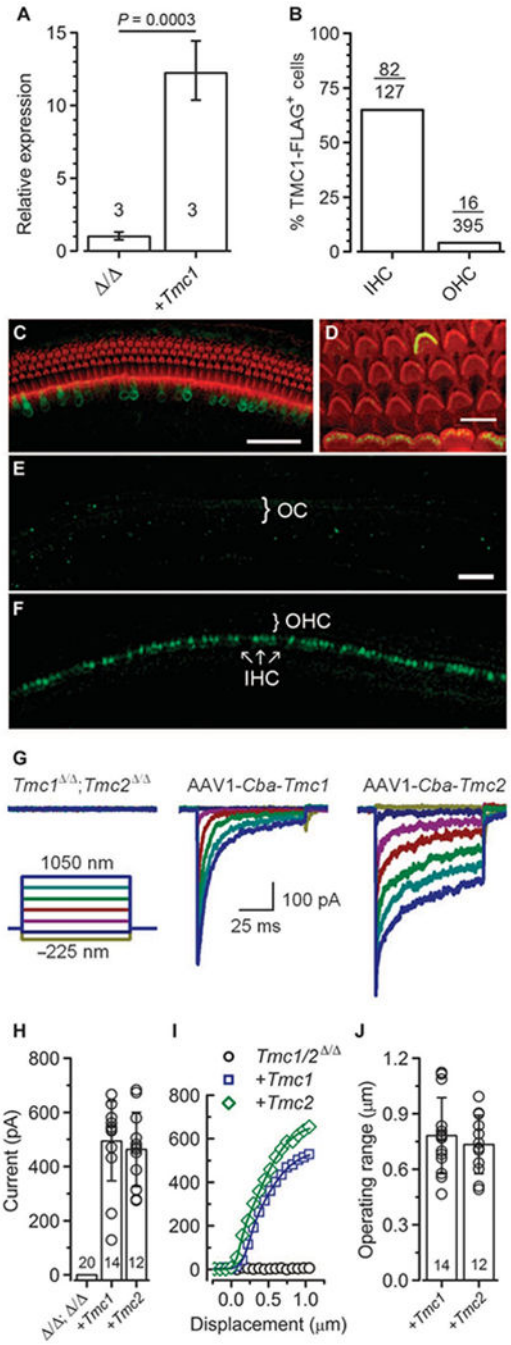

Fig. 3. Exogenous, AAV-delivered *Tmc1/2* restores sensory transduction in *Tmc*-deficient hair cells in vivo.

P0 to P2 *Tmc1*$^{D/D}$;*Tmc2*$^{D/D}$ mice were injected via the RWM with AAV2/1-*Cba-Tmc1* (2.4 × 10^{13} gc/ml) or AAV2/1-*Cba-Tmc2* (1.8 × 10^{13} gc/ml). Cochleas were harvested 6 to 7 days after injection. (A) Quantitative RT-PCR expression analysis of *Tmc1* mRNA from total RNA harvested from two uninjected *Tmc1*$^{D/D}$ cochleas and two *Tmc1*$^{D/D}$ cochleas injected with AAV2/1-*Cba-Tmc1* (*n* = 3 technical replicates). (B) Percent TMC1-FLAG-positive hair cells in AAV2/1-*Cba-Tmc1*-injected cochleas (*n*, number of FLAG-positive cells over total number of cells). (C) Confocal image of a cochlea injected with AAV2/1-

Cba-Tmc1 and stained with Alexa 488 anti-FLAG antibody (green) and Alexa 546–phalloidin (red). Scale bar, 50 mm. (D) Projection from z-stack images of a WT cochlea injected with AAV6/1-*Cba-Tmc2* showing FLAG staining at the tips of hair cell stereocilia. Scale bar, 5 mm. (E and F) FM1-43 uptake in *Tmc1*$^{D/D}$;*Tmc2*$^{D/D}$ tissue not exposed to AAV2/1-*Cba-Tmc* vectors (control; E) or injected (F) with AAV2/1-*Cba-Tmc1.* OC, organ of Corti. Scale bar, 50 mm. (G) Representative families of sensory transduction currents recorded from IHCs of a *Tmc1*$^{D/D}$;*Tmc2*$^{D/D}$ mouse injected with AAV2/1-*Cba-Tmc1* that were FM1-43-negative (left) or FM1-43-positive (middle). FM1-43-positive IHC currents from a *Tmc1*$^{D/D}$;*Tmc2*$^{D/D}$ mouse injected with AAV2/1-*Cba-Tmc2* (right). (H) Peak sensory transduction current amplitudes from FM1-43-negative and FM1-43-positive IHCs of *Tmc1*$^{D/D}$;*Tmc2*$^{D/D}$ mice injected with AAV2/1-*Cba-Tmc1* or AAV2/1-*Cba-Tmc2* as indicated. Bars are means ± SD. Circles are individual measurements (*n*, number of cells). (I) Stimulus-response curves from the currents shown in (G). (J) Ten to 90% operating range measured from stimulus-response curves in (I). Bars are means ± SD. Circles are individual measurements (*n*, number of cells).

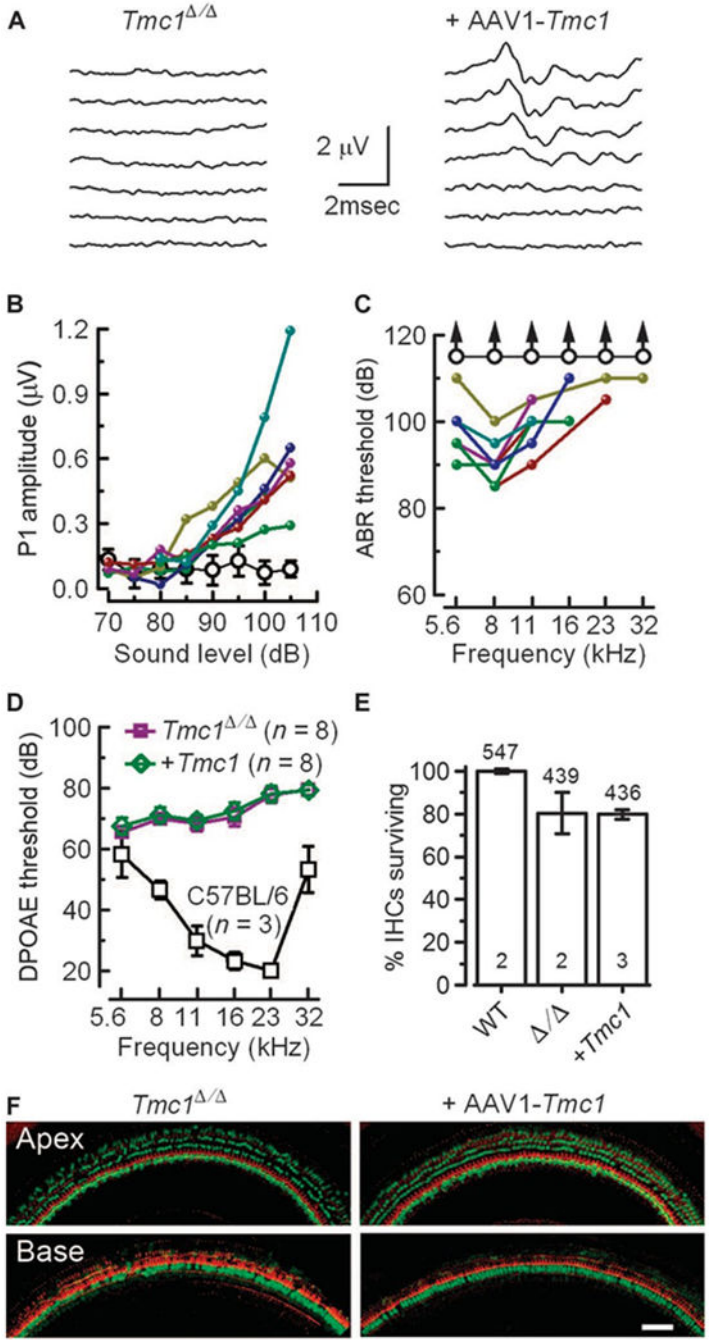

Figure 4: Exogenous *Tmc1* rescues auditory function in *Tmc1*$^{D/D}$ mice.

(A) Families of ABR waveforms recorded from an uninjected *Tmc1*$^{D/D}$ mouse and from a *Tmc1*$^{D/D}$ mouse injected with AAV2/1-*Cba-Tmc1*. ABRs were recorded at P25 to P30 using 8-kHz tone bursts at sound pressure levels between 75 and 105 dB in 5-dB increments. Scale bar applies to both families. (B) Peak 1 amplitudes measured from 8-kHz ABR waveforms, as shown in (A), for eight *Tmc1*$^{D/D}$ mice injected with AAV2/1-*Cba-Tmc1* vectors. Open circles are mean responses (± SD) from uninjected *Tmc1*$^{D/D}$ mice ($n = 8$). (C) ABR thresholds plotted as a function of sound frequency for eight *Tmc1*$^{D/D}$ mice injected with

AAV2/1-*Cba-Tmc1* vectors. Open circles are means of uninjected *Tmc1*$^{D/D}$ mice at the highest sound intensity tested (arrows) (n = 8). (D) DPOAE thresholds as a function of stimulus frequency for WT, uninjected *Tmc1*$^{D/D}$ mice and *Tmc1*$^{D/D}$ mice injected with AAV2/1-*Cba-Tmc1.* Data are means ± SD (n, number of animals). (E) Percentage of surviving IHCs (relative to WT) in 5-mm mid-cochlea sections from *Tmc1*$^{D/D}$ mice and AAV2/1-*Cba-Tmc1*-injected mice (upper n, number of IHCs; lower n, number of cochlea). (F) Confocal images of cochlear whole mounts harvested at P30 from an uninjected *Tmc1*$^{D/D}$ mouse and a *Tmc1*$^{D/D}$ mouse injected with AAV2/1-*Cba-Tmc1.* The tissue was stained for MYO7A (green) and phalloidin (red). Scale bar, 50 mm. Figure S5 shows low-magnification images of the same cochleas.

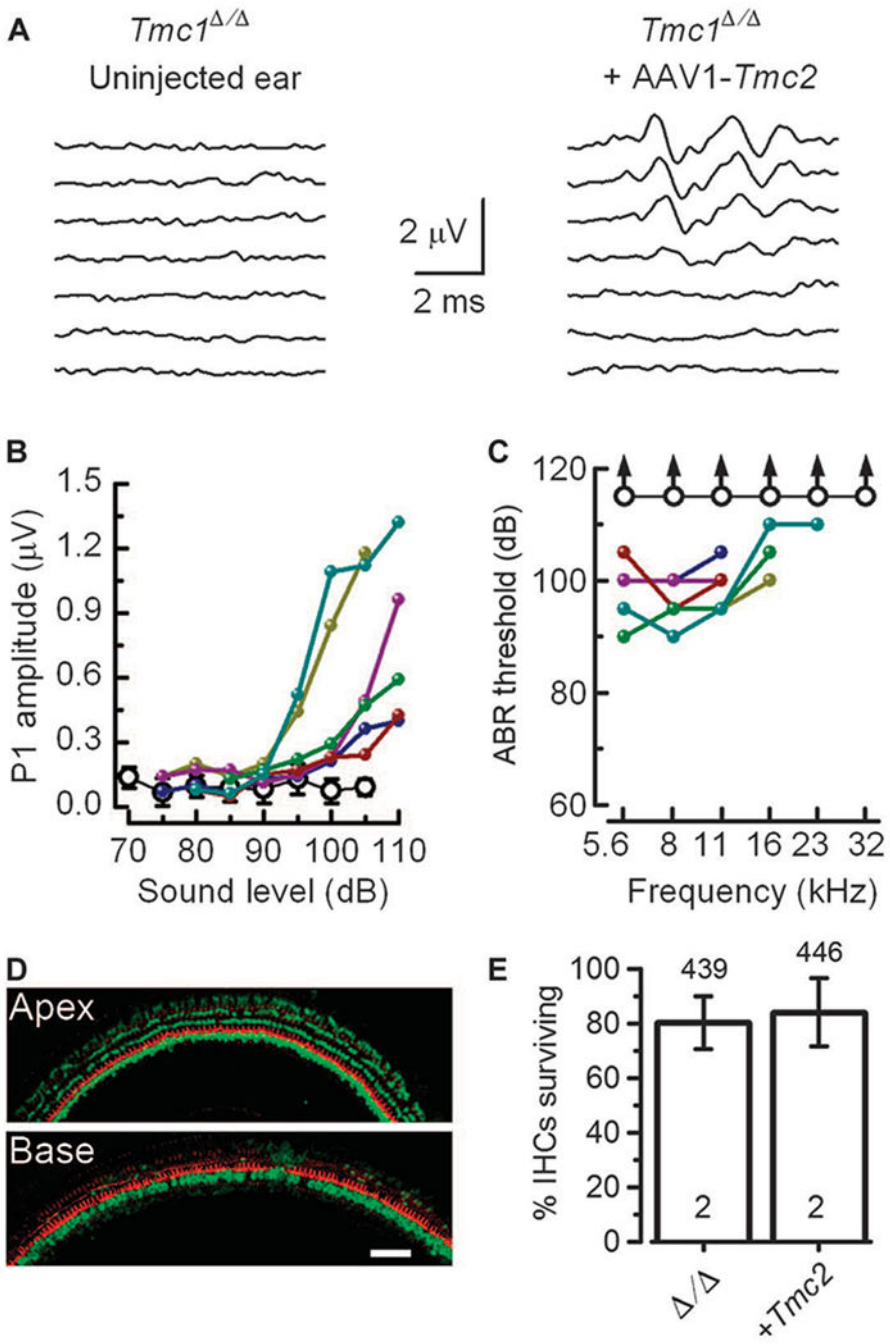

Figure 5: Exogenous *Tmc2* rescues auditory function in *Tmc1*$^{D/D}$ mice.

(A) Families of ABR waveforms recorded from a *Tmc1*$^{D/D}$ mouse injected with AAV2/1-*Cba-Tmc2*. ABRs were recorded at P25 to P30 using 8-kHz tone bursts at sound pressure levels between 75 and 105 dB in 5-dB increments. Scale bar applies to both families. (B) Peak 1 amplitudes measured from 8-kHz ABR waveforms, as shown in (A), for six *Tmc1*$^{D/D}$ mice injected with AAV2/ 1-*Cba-Tmc2* vectors. Open circles are mean responses (±SD) from uninjected *Tmc1*$^{D/D}$ mice (n = 8). (C) ABR thresholds plotted as a function of sound frequency for six *Tmc1*$^{D/D}$ mice injected with AAV2/1-*Cba-Tmc2* vectors. Open circles are

means of uninjected *Tmc1*$^{D/D}$ mice at the highest sound intensity tested (arrows) (n = 8). (D) Confocal images of cochlear whole mounts harvested at P30 from a *Tmc1*$^{D/D}$ mouse injected with AAV2/1-*Cba-Tmc2.* The tissue was stained for MYO7A (green) and phalloidin (red). Scale bar, 50 mm. Figure S5 shows low-magnification images of the same cochleas. (E) Percentage of surviving IHCs in 5-mm mid-cochlea sections from *Tmc1*$^{D/D}$ mice and AAV2/1-*Cba-Tmc2*-injected mice (upper n, number of IHCs; lower n, number of cochleas).

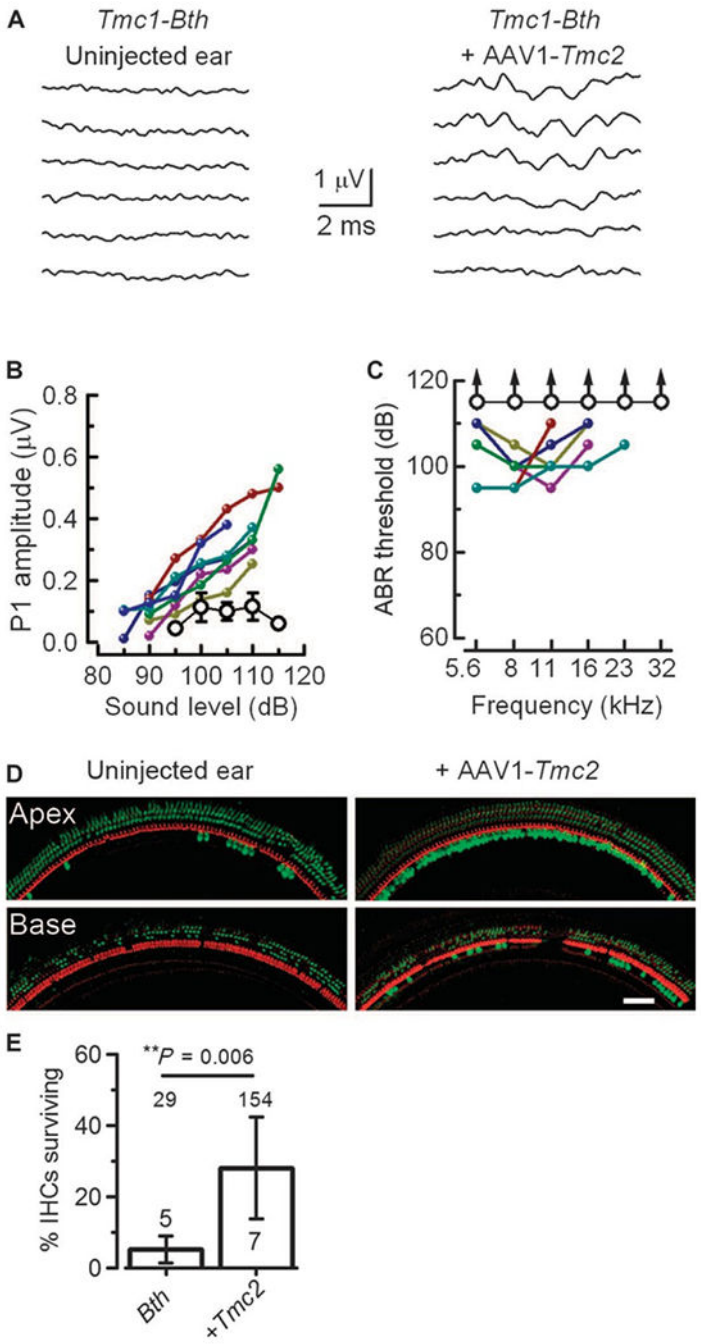

Figure 6: Exogenous *Tmc2* rescues au- ditory function in *Tmc1-Bth* mice.

(A) Families of ABR waveforms recorded from a *Tmc1-Bth* mouse and a *Tmc1-Bth* mouse injected with AAV2/1-*Cba-Tmc2*. ABRs were recorded at P25 to P30 using 8-kHz tone bursts at sound pressure levels between 80 and 110 dB in 5-dB increments. Scale bar applies to both families. (B) Peak 1 amplitudes measured from 8 kHz ABR waveforms, as shown in (A), for seven *Tmc1-Bth* mice injected with AAV2/1-*Cba-Tmc2* vectors. Open circles are mean responses (±SD) from un- injected *Tmc1-Bth* mice ($n = 5$). (C) ABR thresholds plotted as a function of sound frequency for seven *Tmc1-Bth* mice injected with AAV2/1-

Cba-Tmc2 vectors. Open circles are means of uninjected *Tmc1-Bth* mice at the highest sound intensity tested (arrows) ($n = 5$). (D) Confocal images of cochlear whole mounts harvested at P30 from an uninjected *Tmc1-Bth* mouse and a *Tmc1- Bth* mouse injected with AAV2/1-*Cba-Tmc2*. The tissue was stained for MYO7A (green) and phalloidin (red). Scale bar, 100 mm. Note the increased survival of IHCs in the apex and base of the AAV2/1-*Cba-Tmc2* injected cochlea. Figure S6 shows low-magnification images of the same cochleas. (E) Percentage of surviving IHCs in *Tmc1-Bth* mice and AAV2/1-*Cba-Tmc2*– injected *Bth* mice (upper *n*, number of IHCs; lower *n*, number of cochleas).

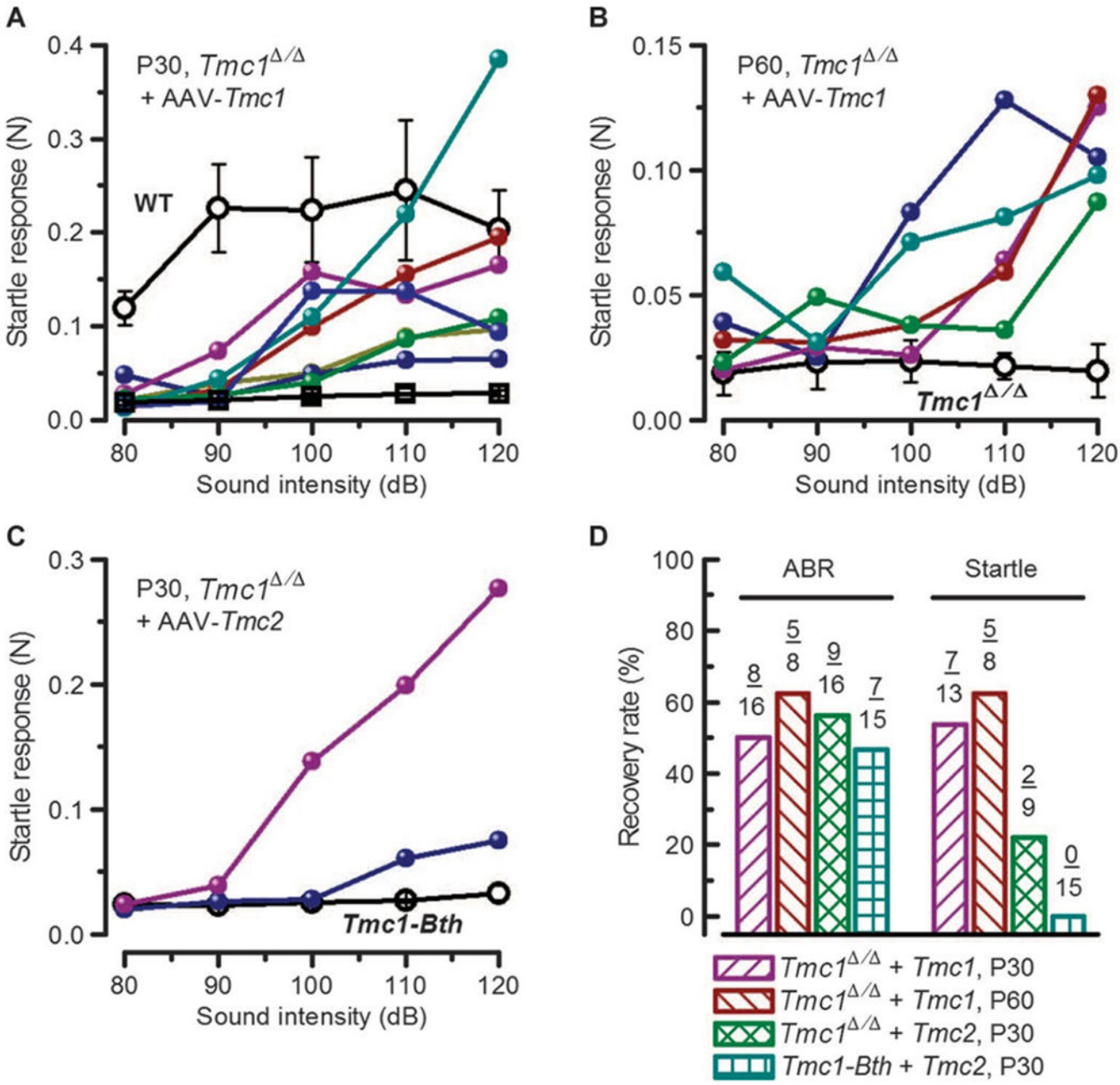

Figure 7: Exogenous *Tmc* expression rescues acoustic startle responses in *Tmc1* mutant mice.

(A) Startle response amplitudes measured at P30 and plotted as a function of sound intensity and as mean ± SD of four control C57BL/6 mice (open circles), seven individual *Tmc1*$^{D/D}$ mice injected with AAV2/1-*Cba-Tmc1*, and five AAV2/1-*Cba-Tmc1*–injected mice with no recovery (open squares). (B) Startle responses measured at P60 and plotted as mean ± SD of four *Tmc1*$^{D/D}$ mice (open circles) and five individual *Tmc1*$^{D/D}$ mice injected with AAV2/1-*Cba-Tmc1*. (C) Startle responses measured at P30, plotted for two individual *Tmc1*$^{D/D}$ mice injected with AAV2/1-*Cba-Tmc2* and as mean ± SD of seven *Tmc1-Bth* mice (open circles) injected with AAV2/1-*Cba-Tmc2*. (D) Summary bar graph showing the percentage of *Tmc1* mutant mice with recovery as assayed by ABRs and startle responses for mice injected with

either AAV2/1-*Cba-Tmc1* or AAV2/1-*Cba-Tmc2.* Numerator indicates *n* mice with recovery of function; denominator indicates *n* injected mice tested. Not all mice were tested with both assays.